Research Article | Vol. 25, No. 23 | 13 Nov 2017 | OPTICS EXPRESS 29000
Optics EXPRESS

Exploiting birefringent thermal lensing effect to manipulate polarization states of an Nd:YVO_4 self-mode-locked laser

P. H. TUAN, M. C. TSAI, AND Y. F. CHEN*

Department of Electrophysics, National Chiao Tung University, 1001, Ta-Hsueh Rd., Hsinchu 30010, Taiwan
yfchen@cc.nctu.edu.tw

Abstract: An Nd:YVO_4 laser with a convex-plano cavity is systematically studied to demonstrate the manipulation of output polarization state by using the birefringent thermal lensing effect of the gain crystal. Based on the theoretical analysis of the cavity stability under the influence of thermal lens, the polarization state of output emission is experimentally confirmed that can be controlled to switch from pure π- to pure σ-polarization by simply varying the pump focus position from the tight-focusing to defocusing conditions. More importantly, it is found that there exists an adequate pump focus position within the switching region to lead the π- and σ-polarization to have balanced gain for achieving a stable self-mode-locked laser with orthogonally polarized components. Under the orthogonally polarized mode-locked operation, the pulse repetition rates are found to be 2.23 and 2.33 GHz for the π- and σ-polarization with pulse duration to be 16.1 and 15.1 ps, respectively.

© 2017 Optical Society of America under the terms of the OSA Open Access Publishing Agreement

OCIS codes: (140.3530) Lasers, neodymium; (350.6830) Thermal lensing; (140.4050) Mode-locked lasers; (140.3480) Lasers, diode-pumped.

References and links

1. F. Krausz, T. Brabec, and C. Spielmann, "Self-starting passive mode locking," Opt. Lett. **16**(4), 235–237 (1991).
2. H. C. Liang, R. C. Chen, Y. J. Huang, K. W. Su, and Y. F. Chen, "Compact efficient multi-GHz Kerr-lens mode-locked diode-pumped Nd:YVO_4 laser," Opt. Express **16**(25), 21149–21154 (2008).
3. A. A. Lagatsky, A. R. Sarmani, C. T. A. Brown, W. Sibbett, V. E. Kisel, A. G. Selivanov, I. A. Denisov, A. E. Troshin, K. V. Yumashev, N. V. Kuleshov, V. N. Matrosov, T. A. Matrosova, and M. I. Kupchenko, "Yb^{3+}-doped YVO_4 crystal for efficient Kerr-lens mode locking in solid-state lasers," Opt. Lett. **30**(23), 3234–3236 (2005).
4. G. Q. Xie, D. Y. Tang, L. M. Zhao, L. J. Qian, and K. Ueda, "High-power self-mode-locked Yb:Y_2O_3 ceramic laser," Opt. Lett. **32**(18), 2741–2743 (2007).
5. H. C. Liang, Y. J. Huang, W. C. Huang, K. W. Su, and Y. F. Chen, "High-power, diode-end-pumped, multigigahertz self-mode-locked Nd:YVO_4 laser at 1342 nm," Opt. Lett. **35**(1), 4–6 (2010).
6. C. Y. Lee, C. C. Chang, H. C. Liang, and Y. F. Chen, "Frequency comb expansion in a monolithic self-mode-locked laser concurrent with stimulated Raman scattering," Laser Photonics Rev. **8**(5), 750–755 (2014).
7. Y. J. Huang, Y. S. Tzeng, C. Y. Tang, and Y. F. Chen, "Efficient dual-wavelength synchronously mode-locked picosecond laser operating on the $^4F_{3/2} \rightarrow {}^4I_{11/2}$ transition with compactly combined dual gain media," IEEE J. Sel. Top. Quantum Electron. **21**(1), 1100107 (2015).
8. A. Schliesser, M. Brehm, F. Keilmann, and D. van der Weide, "Frequency-comb infrared spectrometer for rapid, remote chemical sensing," Opt. Express **13**(22), 9029–9038 (2005).
9. I. Coddington, W. C. Swann, and N. R. Newbury, "Coherent multiheterodyne spectroscopy using stabilized optical frequency combs," Phys. Rev. Lett. **100**(1), 013902 (2008).
10. A. Bartels, R. Cerna, C. Kistner, A. Thoma, F. Hudert, C. Janke, and T. Dekorsy, "Ultrafast time-domain spectroscopy based on high-speed asynchronous optical sampling," Rev. Sci. Instrum. **78**(3), 035107 (2007).
11. N. Kanda, T. Higuchi, H. Shimizu, K. Konishi, K. Yoshioka, and M. Kuwata-Gonokami, "The vectorial control of magnetization by light," Nat. Commun. **2**, 362 (2011).
12. G. D. VanWiggeren and R. Roy, "Communication with dynamically fluctuating states of light polarization," Phys. Rev. Lett. **88**(9), 097903 (2002).
13. X. Yan, J. Liu, J. Su, X. Zhao, and X. Jiang, "Gain competition in orthogonally linearly polarized Nd:YVO_4 laser," J. Opt. **18**, 035201 (2016).
14. H. Huang, D. Shen, and J. He, "Simultaneous pulse generation of orthogonally polarized dual-wavelength at 1091 and 1095 nm by coupled stimulated Raman scattering," Opt. Express **20**(25), 27838–27846 (2012).

#308732 https://doi.org/10.1364/OE.25.029000
Journal © 2017 Received 6 Oct 2017; revised 30 Oct 2017; accepted 2 Nov 2017; published 7 Nov 2017

Optics EXPRESS

15. C. L. Sung, H. P. Cheng, C. Y. Lee, C. Y. Cho, H. C. Liang, and Y. F. Chen, "Generation of orthogonally polarized self-mode-locked Nd:YAG lasers with tunable beat frequencies from the thermally induced birefringence," Opt. Lett. **41**(8), 1781–1784 (2016).
16. M. T. Chang, H. C. Liang, K. W. Su, and Y. F. Chen, "Dual-comb self-mode-locked monolithic Yb:KGW laser with orthogonal polarizations," Opt. Express **23**(8), 10111–10116 (2015).
17. S. V. Sergeyev, C. Mou, A. Rozhin, and S. K. Turitsyn, "Vector solitons with locked and precessing states of polarization," Opt. Express **20**(24), 27434–27440 (2012).
18. Y. Lü, J. Zhang, J. Xia, and H. Liu, "Diode-Pumped Quasi-Three-Level Nd:YVO_4 Laser With Orthogonally Polarized Emission," IEEE Photonics Technol. Lett. **26**(7), 656–659 (2014).
19. B. Xu, Y. Wang, Z. Lin, S. Cui, Y. Cheng, H. Xu, and Z. Cai, "Efficient and compact orthogonally polarized dual-wavelength Nd:YVO_4 laser at 1342 and 1345 nm," Appl. Opt. **55**(1), 42–46 (2016).
20. Z. Lin, Y. Wang, B. Xu, H. Xu, and Z. Cai, "Diode-pumped simultaneous multi-wavelength linearly polarized Nd:YVO_4 laser at 1062, 1064 and 1066 nm," Laser Phys. **26**(1), 015801 (2016).
21. H. C. Liang, F. L. Chang, T. W. Wu, C. L. Sung, and Y. F. Chen, "Generation of Orthogonally Polarized Mode-Locked Lasers at Wavelength of 1342 nm," IEEE Photonics J. **9**(5), 1504908 (2017).
22. A. Agnesi and S. D. Acqua, "High-peak-power diode-pumped passively Q-switched Nd:YVO4 laser," Appl. Phys. B **76**(4), 351–354 (2003).
23. H. C. Liang and C. S. Wu, "Diode-pumped orthogonally polarized self-mode-locked Nd:YLF lasers subject to gain competition and thermal lensing effect," Opt. Express **25**(12), 13697–13704 (2017).
24. Y. Sato and T. Taira, "Highly accurate interferometric evaluation of thermal expansion and *dn/dT* of optical materials," Opt. Mater. Express **4**(5), 876–888 (2014).
25. N. Hodgson and H. Weber, *Laser Resonator and beam propagation*, 2nd ed. (Springer, 2005), Chaps. 8 and 13.
26. W. Koechner, *Solid-State Laser Engineering*, 6th ed. (Springer, 2006), Chap. 7.
27. Y. F. Chen, C. F. Kao, T. M. Huang, C. L. Wang, and S. C. Wang, "Influence of thermal effect on output power optimization in fiber-coupled laser-diode end-pumped lasers," IEEE J. Sel. Top. Quantum Electron. **3**(1), 29–34 (1997).

1. Introduction

The Nd-doped yttrium vanadate (Nd:YVO_4) crystal has long been recognized as a prominent laser host material for diode-pumped solid-state lasers because of its high absorption coefficients and moderate thermal conductivity. Compared with other Nd-doped crystals such as Nd:YAG and Nd:YLF, the Nd:YVO_4 crystal shows the advantages of a higher stimulated emission cross section at 1.06 μm and a stable linearly polarized emission. Besides, the large third-order nonlinearity of the Nd:YVO_4 crystal makes it easy to be exploited to achieve the self-mode-locked (SML) operation whose mechanism is closely related to the nonlinear Kerr lens effect [1, 2]. The SML operation has been proved to be an extremely simple and reliable way to generate mode-locked laser pulses in a short linear cavity [3–7].

Recently, much attention has been paid to study the orthogonally polarized dual-wavelength mode-locked lasers for practical applications including asynchronous optical sampling, control of magnetization, laser spectroscopy, and optical communication [8–12]. To realize an orthogonally polarized dual-wavelength laser [13–17], it is prerequisite to balance the gain-to-loss conditions for the orthogonally polarized states. For a conventional *a*-cut Nd:YVO_4 crystal where the π-polarization (parallel to the crystallographic *c* axis) predominates the laser oscillation, an additional intracavity birefringent element [18–20] or a wedged gain crystal [21, 22] is frequently required to balance the gain competition between the π- and σ-polarization (perpendicular to *c* axis) states. However, such schemes not only make the optical cavity sensitive to misalignment but also increase the intracavity loss which inevitably reduces the output efficiency. Consequently, it will be highly desirable to manipulate the polarization states of an Nd:YVO_4 laser by a more simple and convenient mean for developing the orthogonally polarized mode-locked laser.

It has been reported by Liang *et al.* that an orthogonally polarized mode-locked Nd:YLF laser can be realized without any intracavity element or wedged gain crystal [23]. By simply using the birefringent thermal lensing effect to lead to different stable-cavity conditions for the orthogonally polarized states, the gain-to-loss condition for each polarized state can be adjusted under different pump level. Nevertheless, so far the manipulation of output polarization for the Nd:YVO_4 laser by the thermal lensing is rarely discussed. In this work, an unstable convex-plano cavity is used to demonstrate the manipulation of polarization states

Optics EXPRESS

for a SML Nd:YVO_4 laser. Since a sufficient large thermal lensing effect is mandatory to lead the convex-plano cavity to be stable, the inherent difference of thermal lensing level for the orthogonally polarized emissions of the Nd:YVO_4 crystal can be employed to control the gain-to-loss condition of the polarized states. With theoretical analysis of the cavity stability under the birefringent thermal lensing effect, we find that the laser polarization can be straightforwardly adjusted by varying the pump focus position in the gain crystal. Based on the theoretical results, we experimentally investigate the relationship between the average output power and the pump focus position for the π- and σ-polarization states of a SML Nd:YVO_4 laser. Consistent with the theoretical analysis, it is found that the π-polarization state dominates the laser oscillation under the tight-focusing condition whereas the σ-polarization becomes the dominant state when the pump beam is defocusing. More importantly, between the optimum pump conditions for both the π- and σ-polarization output, there exists an adequate pump focus position that can lead to nearly 1:1 gain balance for the orthogonally polarized states. At the gain-balance pump position, both the π- and σ-polarization can present fairly good fundamental mode locking with the pulse repetition rates to be 2.23 GHz and 2.33 GHz as well as the pulse duration to be 16.1 ps and 15.1 ps, respectively.

2. Cavity stability analysis under the birefringent thermal lensing

For a typical *a*-cut Nd:YVO_4 crystal, the stimulated emission cross section of the π-polarization (25×10^{-19} cm^2) with central emission wavelength at 1064 nm is far larger than that of the σ-polarization (6.5×10^{-19} cm^2) with central emission wavelength at 1066 nm. As a result, the π-polarization state always dominates the laser oscillation in a stable resonator without additional birefringent elements. However, since the σ-polarization have a stronger thermal lensing level because of its larger thermo-optic coefficient compared with that of π-polarization, i.e. $dn_\pi/dT = 8.4\times10^{-6}$ K^{-1} and $dn_\sigma/dT = 15.5\times10^{-6}$ K^{-1} [24], it may become the predominant oscillation state in a thermal-assist-stable resonator which requires a sufficient large thermal lens for stable operation. Throughout this work we consider an unstable convex-plano cavity for demonstration. At first, the stability of the convex-plano resonator under the influence of thermal lensing effect is analyzed to determine the stable criterion for laser oscillation. For an optical resonator with an internal thermal lens, the equivalent *g**-parameter given by [25]

$$g_i^* = \left(1-\frac{L}{R_i}\right)-\frac{d_j}{f_{th}}\left(1-\frac{d_i}{R_i}\right)\ ,\ i,j=1,2\ \&\ i\neq j \tag{1}$$

can be used for the cavity analysis, where f_{th} is the focal length of thermal lens, L is the cavity length, d_1 and d_2 are the optical path length between the mirrors and the incident end face of the gain crystal, and R_i is radius of curvature (ROC) of the cavity mirrors. Note that $d_1 + d_2 = L$ if the thermal lens is assumed to be a thin lens. Considering a convex-plano cavity with $R_1 = -|R|$ and $R_2 \to 0$ then substituting Eq. (1) into the stable condition of $g_1^* g_2^* \le 1$, one can obtain:

$$\frac{d\left(L-d\right)\left(1+d/|R|\right)}{f_{th}^{\ 2}}-\frac{1}{f_{th}}\left(L+\frac{2Ld}{|R|}-\frac{d^2}{|R|}\right)+\frac{L}{|R|}\le 0\quad . \tag{2}$$

Here we define $f_{th,crit}$ as the critical value of focal length for the thermal lens to satisfy Eq. (2). In other words, $f_{th,crit}$ corresponds to the critical thermal lensing that is mandatory to lead the convex-plano cavity to be stable. Note that the negative sign for the convex mirror follows the sign convention for general ABCD law in optics. Here we only consider $g_1^* g_2^* \le 1$ because it plays a more critical condition for the convex-plano resonator. After simple algebra, the

Optics EXPRESS

critical criterion for stable operation of the convex-plano resonator can be solved to be $f_{th,crit} \le |R| + d$. Typically, the gain crystal is fairly close to the front mirror for effective pumping such that $d \approx 0$. Therefore, the critical criterion of $f_{th,crit} \le |R|$ indicates that the thermal lensing level needs to be large enough to compensate the refractive power of the convex mirror for maintaining stable operation.

Next we analyze the thermal lensing effect for the π- and σ-polarization states of the Nd:YVO_4 crystal to validate if the polarization manipulation can be realized in the convex-plano cavity. The effective focal length for the thermal lens of an end-pumped solid-state laser can be approximately modelled as [26]

$$f_{th} = \frac{\pi K_i}{\xi} \frac{\tilde{\omega}_p^{\,2}}{P_{in}} \left[\frac{1}{2} \frac{dn_i}{dT} + \alpha_T \left(n_i - 1 \right) \frac{r_o}{l_c} \right]^{-1}, \tag{3}$$

where K is the thermal conductivity, ξ is the fractional thermal loading, dn/dT is the thermo-optic coefficient, α_T is the thermal expansion coefficient, l_c is the length of gain crystal, r_o is the transverse dimension of gain crystal, P_{in} is the pump power, and $\tilde{\omega}_p$ is the average pump size. The subscript i used here is for denoting the π- or σ-polarization. Note that in Eq. (3) the end effect from the thermal expansion is assumed to be along the cutting axis (a axis) and the term related to thermal stress birefringence is neglected. Since the optical and thermal parameters are solely determined by the gain crystal, Eq. (3) explicitly reveals that the thermal lensing level can be adjusted by varying the pump power or the average pump size. Considering the beam divergence, the average pump size with the pump focus at a distance z_o from the entrance facet of the gain crystal can be expressed as [27]

$$\tilde{\omega}_p(z_o) = \frac{\alpha \int_0^{l_g} \omega_p(z, z_o) e^{-\alpha z} dz}{1 - \exp(-\alpha l_c)} \tag{4}$$

with

$$\omega_p(z, z_o) = \omega_{po} \sqrt{1 + \frac{(z - z_o)^2}{n_i^2 \omega_{po}^2} \theta_p^2}, \tag{5}$$

where α is the absorption coefficient, ω_{po} is the radius of pump beam waist, n is the refractive index, and θ_p is the divergence angle of the pump beam. Since the average pump size directly depends on z_o, the effective focal length of thermal lens can be flexibly altered with different pump focus position in the crystal.

Optics EXPRESS

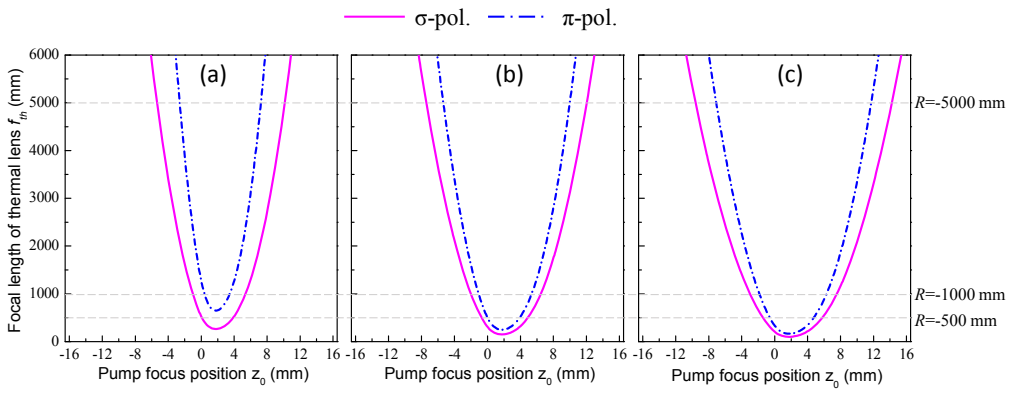

Fig. 1. The effective focal length of thermal lens for the π- and σ-polarization as functions of the pump focus position z_o under the pump power (a) P_{in} = 5 W, (b) P_{in} = 10 W, and (c) P_{in} = 15 W, respectively.

To evaluate the thermal lensing effect for the π- and σ-polarization states of a typical Nd:YVO_4 crystal, Eqs. (3)-(5) are used with the following parameters [24]: $K_\pi = 5.23 \times 10^{-3}$ W·mm^{-1}·K^{-1} and $K_\sigma = 5.10 \times 10^{-3}$ W·mm^{-1}·K^{-1}; $n_\pi = 2.17$ and $n_\sigma = 1.96$; $dn_\pi/dT = 8.4 \times 10^{-6}$ K^{-1} and $dn_\sigma/dT = 15.5 \times 10^{-6}$ K^{-1}; $\alpha = 0.4$ mm^{-1}, $l_c = 10$ mm, $\alpha_T = 1.76 \times 10^{-6}$ K^{-1}, $r_o = 1.5$ mm, and $\xi = 0.24$ which is approximately estimated from the quantum defect. On the other hand, a conventional fiber-coupled laser diode reimaged by a coupling lens set is considered for the pump source with $\omega_{po} = 0.12$ mm and $\theta_p = 0.5$ rad. Figure 1 shows the effective focal length of thermal lenses for the π- (blue chain-dotted line) and σ-polarization (pink solid line) states as functions of the pump focus position z_o under the pump power (a) P_{in} = 5 W, (b) P_{in} = 10 W, and (c) P_{in} = 15 W, respectively. For clearer comparison to the critical criterion of $f_{th,crit} \le |R|$, the gray dotted lines are marked on Fig. 1 to denote the three cases of the convex front mirrors with R = −500, −1000, and −5000 mm. It can be clearly seen that both the thermal lensing levels for π- and σ-polarization states become stronger to lead to larger stable regions of z_o as the pump power increases. Besides, at the region where z_o is far from the tight-focusing point (z_o≈2 mm in these cases), it can be discovered that only the σ-polarization can stably oscillate while the π-polarization is remained unstable. The result indicates that the σ-polarization will be the dominant state under the defocusing pump condition. On the other hand, once the pump focus position is moved to the region close to the tight-focusing point, the π-polarization may deplete all the laser gain and become the dominant oscillation state since it has far larger stimulated emission cross section than that of σ-polarization. The results of the theoretical analysis shed light on the fact that the polarization state of output emission can be successfully switched from π- to σ-polarization when the pump focus position is adjusted from tight-focusing to defocusing region in the convex-plano cavity. In the following section, an Nd:YVO_4 laser experiment with a convex-plano resonator is performed to validate the concept of polarization manipulation by the birefringent thermal lensing effect.

Optics EXPRESS

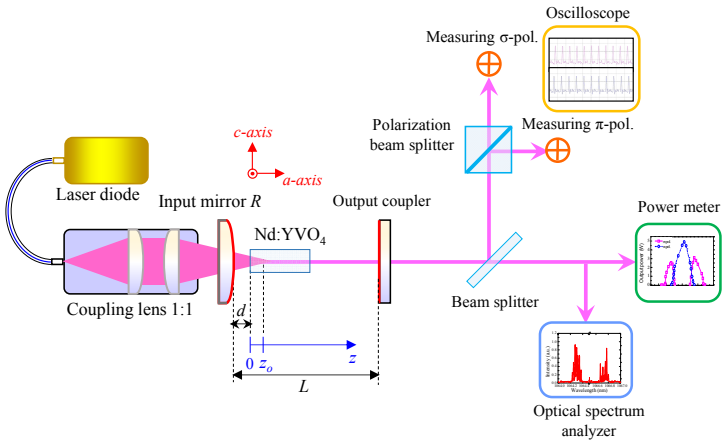

Fig. 2. The experimental setup of the Nd:YVO_4 laser with the convex-plano cavity.

3. Experimental results and discussion

Figure 2 depicts the experimental setup. We used a 0.2 at. % a-cut Nd:YVO_4 crystal as the gain medium. The Nd:YVO_4 crystal with the dimensions of 3 × 3 × 10 mm^3 was coated with antireflection (AR, R<0.1%) at 808 nm and 1064 nm on both end facets and it was placed fairly closed to the input mirror with $d \approx 0$ for effective pumping. The laser crystal was wrapped with indium foil and mounted in water-cooled copper heat sinks at 16°C. The pump source was a 20-watt fiber-coupled laser diode at 808 nm with a core diameter of 200 μm and a numerical aperture of 0.16 combined with a reimaging lens set with an effective focal length of 25 mm. The pump beam was reimaged into the gain crystal with a focal beam radius $\omega_{po} \approx 120$ μm considering the beam divergence. For obtaining a suitable operation range of z_o to manipulate the output polarization as well as maintaining a good matching condition between the pump and lasing mode, we chose a convex mirror with R = −1000 mm as the input mirror according to the theoretical analysis. The input mirror was coated AR at 808 nm on the entrance face as well as high-transmittance (HT, T>95%) at 808 nm and high-reflectance (HR, R>99.9%) at 1064 nm at the second facet. A plane mirror with 8% transmission at the wavelengths of 1064 nm and 1066 nm was used as the output coupler. The geometric cavity length was set to be L = 53 mm for achieving a good self-mode-locked operation [2]. A Michelson optical spectrum analyzer (Advantest, Q8347) was employed to monitor the lasing spectrum with a resolution of 0.003 nm. The temporal behavior of the laser output was detected by a high-speed InGaAs photodetector (Electro-Optics Technology Inc. ET-3500 with rise time 35 ps), whose output signal was connected to a digital oscilloscope (Lecroy 820Zi-A) with 20 GHz and a sampling interval of 25 ps.

Optics EXPRESS

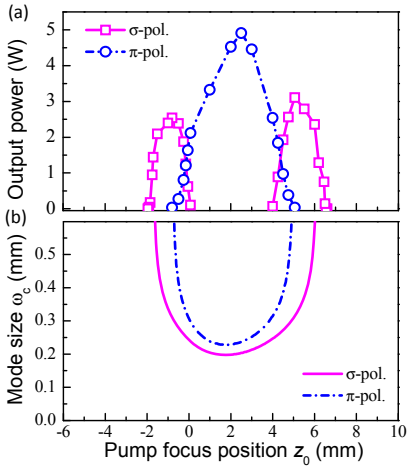

Fig. 3. (a) The average output power and (b) the cavity mode size on the gain medium for the π- and σ-polarization versus the pump focus position z_o under an incident pump power P_{in} = 10 W.

At first the dependence of average output power for the π- and σ-polarization on the pump focus position z_o was examined to verify the theoretical prediction. Figure 3(a) shows the results of output power for the π- and σ-polarization versus z_o under a fixed incident pump power P_{in} = 10 W. For easier comparison, the cavity mode size on the gain crystal ω_c as a function of z_o for each polarized emission under the thermal lensing effect was calculated by [24]

$$\omega_c = \sqrt{\frac{\lambda L^*}{\pi}\sqrt{\frac{g_2^*}{g_1^*(1-g_1^*g_2^*)}}\left[\left(1-\frac{d_1}{R_1}\right)^2+\left(\frac{d_1}{L^*}\right)^2\frac{g_1^*(1-g_1^*g_2^*)}{g_2^*}\right]} \tag{6}$$

and shown as Fig. 3(b) to clearly present the region of z_o for stable operation. Here $L^* = d_1 + d_2 - (d_1 d_2)/f_{th}$ is the effective cavity length. Consistent with the theoretical analysis, the experimental results show that the σ-polarization dominates the output emission at the region of z_o to which it can be exclusively stable under the defocusing condition; while the π-polarization becomes the dominant state once the pump condition can lead it to be stable. In this case, the maximum output power for the π- and σ-emission can be found to be 5.0 W and 3.1 W at the pump positions approximately to be z_o = 2.5 and 5 mm, respectively. More intriguingly, it can be discovered that there exists adequate pump positions within the switching regions between π- and σ-emission to lead the orthogonally polarized states to be gain-balanced. The gain-balanced operation is prerequisite for achieving a good dual-wavelength orthogonally polarized laser. We then adjust the pump focus to the optimum positions for the π-, σ-, and dual-polarization emission to investigate the output efficiency of the Nd:YVO_4 laser. Figures 4(a)-4(c) show the average output power versus the incident pump power for the cases of π-, σ-, and dual-polarization emission at the pump focus positions z_o≈2.5, 4.4, and 5 mm, respectively. At the incident pump power of 17.5 W, the average output power of the pure π- and σ-polarization emission can reach 8.5 W and 5.1 W with the optical-to-optical conversion efficiency to be 48.6% and 29% as well as the slope efficiency approximately to be 50% and 33%, respectively. For the case of dual-polarization emission, it can be seen that the average output power for the π- and σ-polarization can be maintained to be nearly 1:1 with almost the same slope efficiency when the pump power is far higher than the threshold power. At the incident pump power of 17.5 W, the total output

Optics EXPRESS

power of the dual-polarization emission can reach 5.0 W with an optical-to-optical conversion efficiency to be 28.6%.

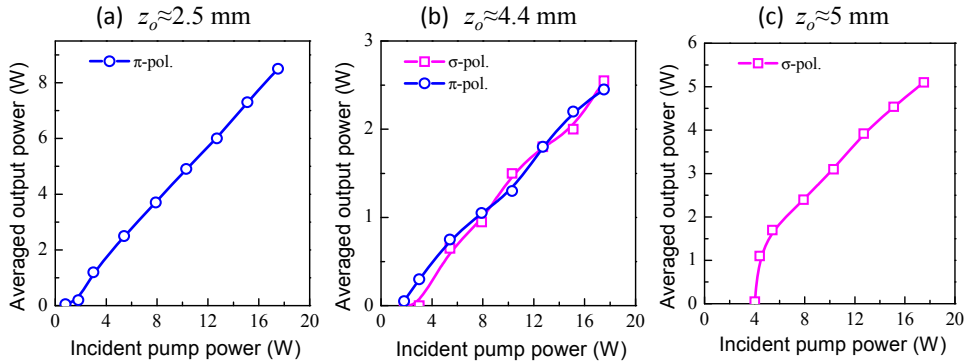

Fig. 4. The average output power versus the incident pump power for the cases of π-, σ-, and dual-polarization emission at their optimum pump positions of (a) 2.5, (b) 4.4, and (c) 5 mm.

Next the spectral information and the temporal behaviors of the orthogonally polarized Nd:YVO_4 laser are further measured for the cases of π-, σ-, and dual-polarization emission to explore the self-mode-locked (SML) operation. The stable SML operation associated with the nonlinear optical effect has been reported that can be frequently observed in lasers with a short linear cavity [4–6]. Figures 5(a)-5(d) show the optical spectrum, the oscilloscope trace, the RF spectrum, and the second-order autocorrelation trace for the case of pure π-polarization emission under a pump power of 10 W. From the optical spectrum as shown in Fig. 5(a), it can be seen that the central wavelength of the lasing modes locates at 1064.4 nm with an optical spectral width approximately to be 0.14 nm. The temporal trace shown in Fig. 5(b) with the time span of 5 ns reveals that all the lasing modes can be coherently locked to achieve a stable SML operation with a pulse repetition rate to be 2.23 GHz that is consistent with the round-trip time given by the optical cavity length of 64.4 mm. The overall amplitude fluctuation of the mode-locked pulses in this case is found to be less than 2%. The power spectrum measured by the RF spectrum analyzer (Agilent, 8563EC) in a span of 8 GHz with a resolution bandwidth of 300 kHz is provided to further confirm the stability of the SML operation as shown in Fig. 5(c). It can be observed that the peaks at 2.23, 4.46, and 6.69 GHz well correspond to the fundamental, 2nd-harmonic, and 3rd-harmonic frequency of the free spectral range. Furthermore, the amplitudes of the signal to noise for the fundamental and 2nd-harmonic peaks are nearly up to 50 dBm indicating a fair good SML operation. The pulse duration of the SML laser can be estimated from the second-order autocorrelation trace measured by a commercial autocorrelator (APE pulse check, Angewandte Physik & Elektronik GmbH) to be 16.1 ps under a Gaussian-shaped assumption as shown in Fig. 5(d). The transverse pattern of the SML laser was also shown as the inset of Fig. 5(d) to confirm a good fundamental mode operation.

Optics EXPRESS

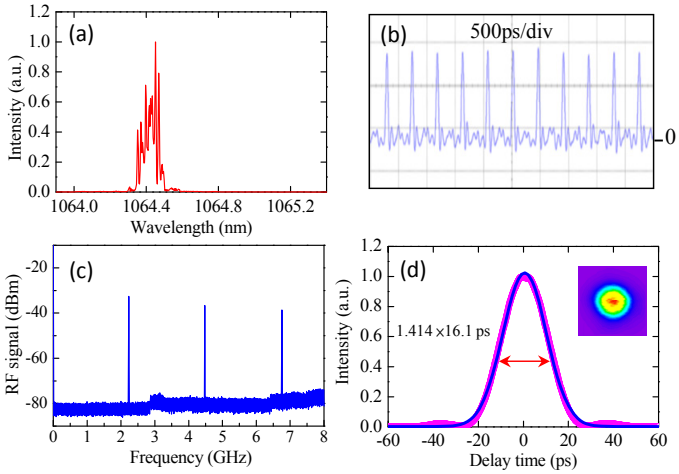

Fig. 5. (a) The optical spectrum, (b) the oscilloscope trace with time span of 5 ns, (c) the RF spectrum, and (d) the second-order autocorrelation trace measured at P_{in} = 10 W for the Nd:YVO_4 SML laser with pure π-polarization. The inset of (d) shows the transverse pattern.

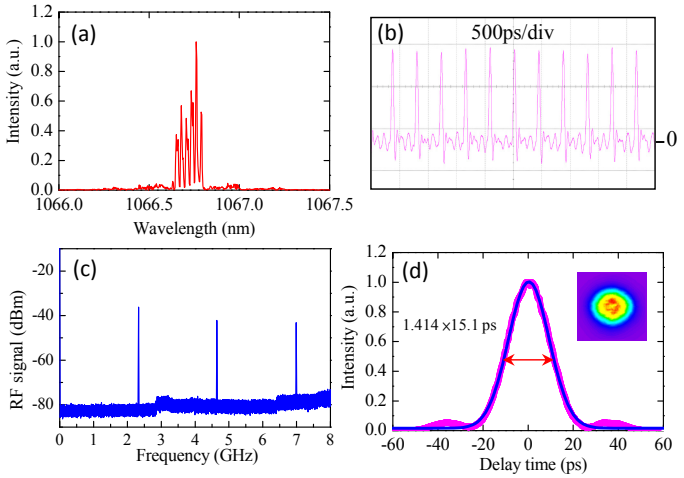

Fig. 6. (a) The optical spectrum, (b) the oscilloscope trace with time span of 5 ns, (c) the RF spectrum, and (d) the second-order autocorrelation trace measured at P_{in} = 10 W for the Nd:YVO_4 SML laser with pure σ-polarization. The inset of (d) shows the transverse pattern.

We then adjusted the pump focus to the optimum position for σ-polarization emission to measure its spectral and temporal properties. Figures 6(a)-6(d) depict similar plots as those of Figs. 5(a)-5(d) but for the σ-polarization. The central wavelength of the pure σ-polarization emission was at 1066.7 nm as shown in Fig. 6(a). The optical spectral width can be estimated to be 0.14 nm which is similar to the case of π-polarization. The SML pulse train with a pulse repetition rate of 2.33 GHz and an amplitude fluctuation less than 3% can also be measured in this case as seen from Fig. 6(b). For the RF spectrum shown in Fig. 6(c), the signal-to-noise amplitude of the fundamental and 2nd-harmonic peaks can be found to be nearly 40 dBm that is good enough for a stable SML operation. The pulse duration for the SML laser with pure σ-polarization was found to be 15.1 ps under a Gaussian-shaped fitting as seen from the second-order autocorrelation trace shown in Fig. 6(d). Besides, the transverse pattern of the lasing mode shown by the inset of Fig. 6(d) was also confirmed to correspond to a good fundamental mode operation.

Optics EXPRESS

Finally, the pump focus condition was adjusted to the optimum position for the dual-polarization emission. The optical spectrum shown in Fig. 7(a) reveals that the output intensity of the π- and σ-polarization states can be maintained to be nearly 1:1 with similar spectral bandwidth to be 0.14 nm. Meanwhile, the output transverse patterns shown by the insets of Fig. 7(a) exhibit both the orthogonally polarized states can sustain good fundamental mode operation simultaneously. As a consequence, the stable SML pulse trains with the amplitude fluctuation less than 3% can be measured for both the π- and σ-polarization in this case as shown in Fig. 7(b). The RF spectrum and the second-order autocorrelation trace for each polarization state in this case have been confirmed to be nearly the same as those for the case of pure polarization emission. The experimental results not only validate that the polarization manipulation of an Nd:YVO_4 laser can be successfully realized by using the birefringent thermal lensing effect with the convex-plano cavity design but also offer an simple and convenient approach to achieve an orthogonally polarized mode-locked laser for further applications.

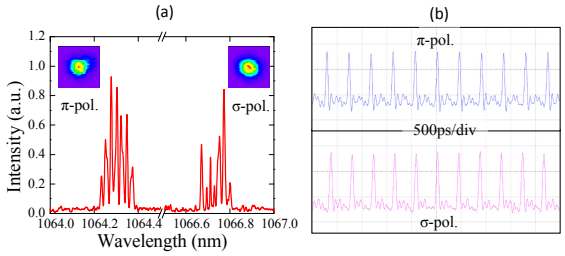

Fig. 7. (a) The optical spectrum and (b) the SML pulse trains of the Nd:YVO_4 laser with 1:1 dual-polarization components. The insets of (a) show the transverse patterns of the π- and σ-components, respectively.

4. Conclusion

In conclusion, an Nd:YVO_4 laser with a convex-plano cavity design has been thoroughly investigated to demonstrate the manipulation of polarization states by using the birefringent thermal lensing effect. We have theoretically analyzed the cavity stability under the birefringent thermal lensing effect to find that the laser polarization state can be straightforwardly controlled by adjusting the pump focus position in the gain crystal. To verify the theoretical analysis, the relationship between the output polarization state and the pump focus position have been experimentally studied to find that a stable SML operation with pure π-polarization or pure σ-polarization can be respectively observed under the tight-focusing or defocusing condition. More importantly, it have been discovered that there exist adequate pump positions within the switching regions between π- and σ-polarization that can lead both the orthogonally polarized states to reach the gain-balanced condition. At the gain-balanced pump position, a stable orthogonally-polarized SML laser with the pulse repetition rates to be 2.23 GHz and 2.33 GHz as well as the pulse duration to be 16.1 ps and 15.1 ps respectively for the π- and σ-components can be successfully achieved. It is worthy to mention that the proposed configuration and approach for manipulating output polarization via the birefringent thermal lensing may be generalized to other gain crystals with a sufficient large difference of thermal lensing levels for the orthogonally polarized states. Nevertheless, it requires more detailed theoretical analyses and experiments to find out the optimum parameters of the gain crystals such as doping concentration, geometry dimensions, and so on for further improving the stability of the orthogonally-polarized SML operation.

Funding

Ministry of Science and Technology of Taiwan (Contract No. MOST-105-2628-M-009-001).

136.233.64.150 {ts '2018-08-01 14:55:55'}